Journal of Scientific & Industrial Research
Vol. 79, October 2020, pp. 883-889

Effects of the Sensors Arrangement on the Efficiency of Multi-Transmitter and Multi-Receiver Passive Radar

Saeed Fooladi Talari* and Kamal Mohamedpour
Faculty of Electrical Engineering, KNToosi University of Technology, Tehran, Iran

Received 18 February 2020; revised 4 March 2020; accepted 14 July 2020

Passive radar is of interest in many aspects. These radars accomplish target localization by receiver sensors. In this paper, we investigate the effect of the sensors arrangement on the performance of multi-transmitter and multi-receiver passive radar and present a method to maximize target localization accuracy on the important locations by the optimal arrangement of receiver sensors. The proposed method is based on the Cramer-Rao lower band. The optimal placement of receiver sensors can be achieved with the help of the proposed method. We investigate the types of sensors arrangement for better accuracy in the surveillance area. The provided Cramer-Rao lower band is developed for the use of time difference of arrival measurements and the angle of arrival measurements. As illustrated in the simulations results, the joint use of both the time difference of arrival and the angle of arrival is better than the use of them alone. Furthermore, the blind areas caused by the receiver sensors arrangement are eliminated by the joint use of measurement. On the other hand, the target localization efficiency increases with the increasing distance between sensors and their dispersion in the environment.

Keywords: Localization, Multi-Transmitter Multi-Receiver Radar, Passive Radar, Sensors Arrangement

Introduction

Radars detect targets by receiving electromagnetic radiation emitting from them. While active radars use signal transmission and reflection reception to detect targets. Passive radars use the reflected signals of the opportunistic transmitters from the target to localize it. The use of opportunistic transmitters makes the passive radar invisible in the electromagnetic spectrum. This property of passive radars has drawn the attention to this technology in the military field. On the other hand, since these radars do not need to transmit signals, the transmitter module and frequency allocation are not required in the passive radars. This property has attracted attention in the commercial field.[1–7]

Various types of opportunistic transmitters have been investigated for passive radar. These transmitters are classified into terrestrial and satellite categories. On the other hand, transmitters are classified into two types of broadcast transmitters and communication network transmitters. Terrestrial broadcast signals such as FM, DAB, DVB-T[8], terrestrial communication networks such as GSM, 3G, and 4G[9], Wi-Fi signal[10], and satellite signal such as GNSS[11] have been investigated for use as opportunistic transmitters.

Signal processing for passive radars is similar to the bistatic or multi-static radars. The transmitter and receiver are geographically separated in such radars. In bistatic passive radar, it is necessary to receive the signals of transmitters and target reflection, simultaneously. By extending the bistatic radar to multi-static by increasing the number of transmitters and/or receivers, it is possible to localize the target by the passive radar.[12–16] Scenarios of signal processing using just reflected signals are possible too. In these scenarios, there is no need for receiving the transmitter signals, while detection and localization can only be performed using the target reflected signals.[17,18]

In this paper, we investigate the effect of receiver sensors arrangement on the performance of the passive radar. A procedure for evaluating target localization performance has been provided.[19] We use the same procedure for target localization in the scenario of passive multi-transmitter multi-receiver radar localization. The decentralized scenario of signal processing is considered in receiver sensors. It is assumed that the receiver sensors can obtain TDOA and AOA measurements by processing the reflected signals from the target. The AOA measurements are

*Author for Correspondence
E-mail: s.fooladi@ee.kntu.ac.ir

obtained by processing of received signals from the antenna array, while the TDOA measurements are obtained by simultaneous processing of received-reflected signals from the target and the transmitters signals. The efficiency of the target location estimation by the number of receiver sensors is provided for the combined use of TDOA and AOA measurements and the use of them alone. The transmitter network is considered MFN (i.e. transmitters use different frequencies), and the target reflected signals can be separated for the different transmitters in the receiver.

The performance of target localization and evaluating the effect of sensors arrangement is provided by the Cramer-Rao lower band (CRLB) of the target location estimation independent of signal. Simulation results show the advantages and disadvantages of using the measurements and the type of arrangement.

Experimental Details

System Model

The passive radar employs available transmitters in the environment to target localization. The bistatic processing of the reflected signals received from the target needs to receive the reference signals of transmitters. The geographical scheme of the passive radar includes M opportunistic transmitters that continuously emitting their signals in the environment. The passive radar's N receiver sensors use two separate channels to receive reference signals of the transmitters and reflected signals of the target. After calculating the TDOA and AOA measurements in the receiver sensors, these measurements are sent to the central sensor to estimate the target location. In this section, we will present the signal and measurement models.

Signal Model

The receiver sensors use two separate channels to receive the transmitter signals and the target reflections, which are called the direct and surveillance channels, respectively. The reference signal of the transmitter is received by a directional antenna, aligned to the transmitter's direction. The target echoes are received by an array of omnidirectional antennas. The target direction finding is made by the signals processing of the array antenna. The time difference of arrival is calculated by the bistatic processing of the reference signal and surveillance signal.

The location of the transmitters and receivers are indicated by $\underline{p}_{Tx_i} = [x_{Tx_i} y_{Tx_i} z_{Tx_i}]^T$ and $\underline{p}_{Rx_j} = [x_{Rx_j} y_{Rx_j} z_{Rx_j}]^T$, respectively, where i is the transmitter number index and j is the receiver number index. The target is in $\underline{p}_{Ta} = [x_{Ta} y_{Ta} z_{Ta}]^T$. The received direct path signal and the received reflected signal at the receiver j that is emitting from the transmitter i are presented in Eqs (1) and (2).

$$sr_{Tx_i-Rx_j}(t) = (1/g_{Tx_i-Rx_j}) s_{Tx_i}(t - \tau_{Tx_i-Rx_j}) a(\theta_{Tx_i-Rx_j}.\varphi_{Tx_i-Rx_j}) \quad \ldots (1)$$

$$ss_{Tx_i-Ta-Rx_j}(t) = (1/g_{Tx_i-Ta-Rx_j}) s_{Tx_i}(t - \tau_{Tx_i-Ta-Rx_j}) a(\theta_{Ta-Rx_j}.\varphi_{Ta-Rx_j}) \quad \ldots (2)$$

where $s_{Tx_i}(t)$ is the transmitted signal, $sr_{Tx_i-Rx_j}(t)$ is the received direct path signal, $ss_{Tx_i-Ta-Rx_j}(t)$ is the received reflected signal, $g_{Tx_i-Rx_j}$ is the direct path signal attenuation, $\tau_{Tx_i-Rx_j}$ is the delay of direct path signal, $a(\theta_{Tx_i-Rx_j}.\varphi_{Tx_i-Rx_j})$ indicates angular function of transmitter in the receiver sensor location, $g_{Tx_i-Ta-Rx_j}$ is the reflected signal's attenuation, $\tau_{Tx_i-Ta-Rx_j}$ is the time delay of reflected signal, and $a(\theta_{Ta-Rx_j}.\varphi_{Ta-Rx_j})$ indicates angular function of target in the receiver sensor location. The symbols θ and φ indicate azimuth angle and elevation angle, respectively.

We ignore the attenuation parameters due to the calculation of TDOA and AOA measurements at the receiver. The delays and the angle parameters calculated in the receiver sensors are presented in Eqs (3–6).

$$\tau_{Tx_i-Rx_j} = r_{Tx_i-Rx_j}/c \quad \ldots (3)$$

$$\tau_{Tx_i-Ta-Rx_j} = (r_{Tx_i-Ta} + r_{Ta-Rx_j})/c \quad \ldots (4)$$

$$\theta_{Ta-Rx_j} = \text{atan}\left((y_{Ta} - y_{Rx_j})/(x_{Ta} - x_{Rx_j})\right) \quad \ldots (5)$$

$$\varphi_{Ta-Rx_j} = \text{asin}\left((z_{Ta} - z_{Rx_j})/r_{Ta-Rx_j}\right) \quad \ldots (6)$$

Where $r_{a-b} = ||\underline{p}_a - \underline{p}_b||$ is the distance between $\underline{p}_a$ and $\underline{p}_b$ locations, $||\underline{x}||$ indicates the norm of $\underline{x}$ vector, and c is the signal propagation speed. The power of the received reflected signal is inversely related to the square of the range of target (i.e. $p_{ss_{Tx_i-Ta-Rx_j}} \sim {r_{Ta-Rx_j}}^2$).[19]

Measurements Model

As mentioned above, after calculating the TDOA and AOA measurements in the receiver sensors by the

signal processing, the calculated measurements in the receiver sensors are sent to the central sensor to the target location estimation. The vector of the measurements is shown by $\underline{k} = [\underline{\tau}^T \underline{\theta}^T \underline{\varphi}^T]^T$. Where $\underline{k}$ is the vector of all measurements, $\underline{\tau}$, $\underline{\theta}$, and $\underline{\varphi}$ are vector of the TDOA measurements, vector of the azimuth angle of DOA measurements, and vector of the elevation angle of DOA measurements, respectively. The delay between the reflected signal and the direct path signal is calculated using the CAF processing of them. The delay between the transmitter's direct path signal and the target's reflected signal is denoted by $\tau_{Tx_i-Ta-Rx_j.Tx_i-Rx_j}$ and equal to $\tau_{Tx_i-Ta-Rx_j} - \tau_{Tx_i-Rx_j}$. The locations of the transmitters and receiver sensors are known. Therefore, the $\tau_{Tx_i-Rx_j}$ can be calculated easily. Therefore, $\tau_{Tx_i-Ta-Rx_j}$ can be calculated by the calculation of $\tau_{Tx_i-Ta-Rx_j.Tx_i-Rx_j}$ and $\tau_{Tx_i-Rx_j}$. The $\underline{\tau}$ vector includes the bistatic delays ($\tau_{Tx_i-Ta-Rx_j}$). The $\underline{\theta}$ and $\underline{\varphi}$ vectors also contain the measured azimuth angles and elevations angles ($\theta_{Ta-Rx_j}.\varphi_{Ta-Rx_j}$), respectively, that are calculated in the receiver sensors. These angles are obtained by the array processing of signals of the antenna array in the receiver sensors.

The measurements vector is easily reducible for the cases not using the one type of measurements. The calculation of these measurements is accompanied by noise, which we model as additive noise. For simplicity of calculations, we consider measurements' noises as additive white Gaussian noises. Therefore, the measured vector is equal to $\underline{k} = \underline{k}^o + \underline{n}_{\underline{k}}$, where the vector $\underline{k}$ represents the noisy measurements, $\underline{k}^o$ represents the actual values, and $\underline{n}_{\underline{k}} \sim N(0.Q)$ is the noise vector that $diag(Q) = [\underline{\sigma}_\tau{}^{2T} \underline{\sigma}_\theta{}^{2T} \underline{\sigma}_\varphi{}^{2T}]^T$. Where, $\underline{\sigma}_\tau{}^2$, $\underline{\sigma}_\theta{}^2$, and $\underline{\sigma}_\varphi{}^2$ are the vector of noise variances of TDOA measurements, the azimuth angles of DOA measurements, and the elevation angles of DOA measurements, respectively. Other measurement cases are obtained by simplifying and reducing these vectors. Other possible modes including TDOA only and AOA only can be achieved by deleting the unused information vector.

Performance of Target Localization

As mentioned above, the TDOA and AOA measurements are sent to the central sensor to estimate the target location. Target location estimation is calculated based on the known location of the transmitters and receiver sensors and calculation of the measurements vector. We use the performance lower band of target location estimation (CRLB) to investigate the effect of the sensors arrangement on the performance of target location estimation. By the MFN assumption of opportunistic transmitter networks, the reflected signals from the target can be separated for each opportunistic transmitter. Therefore, a TDOA measurement and a DOA measurement for azimuth and elevation angles can be calculated for each opportunistic transmitter. As a result, we will have $M \times N$ numbers of TDOA and DOA measurements in a network consisting of M transmitters by N receiver sensors. The $\underline{\tau}$, $\underline{\theta}$, and $\underline{\varphi}$ are shown in Eq. (7).

$$\begin{aligned}\underline{\tau} &= [\tau_{Tx_1-Ta-Rx_1} \dots \tau_{Tx_1-Ta-Rx_N} \dots \tau_{Tx_M-Ta-Rx_N}]^T \\ \underline{\theta} &= [\theta_{Ta-Rx_1|Tx_1} \dots \theta_{Ta-Rx_N|Tx_1} \dots \theta_{Ta-Rx_N|Tx_M}]^T \\ \underline{\varphi} &= [\varphi_{Ta-Rx_1|Tx_1} \dots \varphi_{Ta-Rx_N|Tx_1} \dots \varphi_{Ta-Rx_N|Tx_M}]^T \end{aligned} \quad \dots (7)$$

According to the Gaussian assumption of noises, we obtain the CRLB by calculating the Fisher matrix of information corresponding to the measurements used and independent of the signal features. The CRLB matrix of $\underline{p}_{Ta}$ is $CRLB\left(\underline{p}_{Ta}\right) = FIM^{-1}\left(\underline{p}_{Ta}\right)$.[20] The FIM matrix represents the Fisher information matrix. According to the Gaussian assumption of noises, the Fisher matrix of measurements is equal to $FIM\left(\underline{p}_{Ta}\right) = (\partial k/\partial p_{Ta}{}^T)^T Q^{-1} (\partial \partial k/\partial p_{Ta}{}^T)$

$FIM\left(\underline{p}_{Ta}\right) = \left(\partial \underline{k}/\partial \underline{p}_{Ta}{}^T\right)^T Q^{-1} (\partial \partial \underline{k}/\partial \underline{p}_{Ta}{}^T)$ .Where, Q is the covariance matrix of measurements and $\partial \underline{k}/\partial \underline{p}_{Ta}$ represents the derivative of the measurements vector relative to the target location. $\partial \underline{k}/\partial \underline{p}_{Ta}{}^T$ for TDOA measurements and AOA measurements are presented in Eq. (8).

$$\frac{\partial \tau_{Tx_i-Ta-Rx_j}}{\partial \underline{p}_{Ta}{}^T} = c^{-1}\left[(\underline{p}_{Ta} - \underline{p}_{Tx_i})/r_{Tx_i-Ta} + (\underline{p}_{Ta} - \underline{p}_{Rx_j})/r_{Ta-Rx_j}\right]^T$$

$$\frac{\partial \theta_{Ta-Rx_j}}{\partial \underline{p}_{Ta}{}^T} = (l_{Ta-Rx_j}{}^2)^{-1}\left[\left(\left[\underline{p}_{Ta} - \underline{p}_{Rx_j}\right]^T \underline{x}\right)\underline{y} - \left(\left[\underline{p}_{Ta} - \underline{p}_{Rx_j}\right]^T \underline{y}\right)\underline{x}\right]^T$$

$$\frac{\partial \theta \varphi_{Ta-Rx_j}}{\partial \underline{p}_{Ta}{}^T} =$$

$$(r_{Ta-Rx_j}{}^2 l_{Ta-Rx_j})^{-1}\left[\left(\left[\underline{p}_{Ta}-\underline{p}_{Rx_j}\right]^T \underline{z}\right)\left[\underline{p}_{Ta}-\underline{p}_{Rx_j}\right]+r_{Ta-Rx_j}{}^2\underline{z}\right]^T \quad \ldots (8)$$

where $l_{Ta-Rx_j}=\sqrt{(\underline{x}_{Ta}-\underline{x}_{Rx_j})^2+(\underline{y}_{Ta}-\underline{y}_{Rx_j})^2}$, $\underline{x}=[1\ 0\ 0]^T$, $\underline{y}=[0\ 1\ 0\ ]^T$, and $\underline{z}=[\ 0\ 0\ 1]^T$.

Using the presented CRLB, we can calculate the performance of target localization for different locations for utilizing TDOA measurements or AOA measurements or both.

Results and Discussion

Effective Parameters

SNR

The accuracy of the measurements is directly related to the SNR of the received signal at the receiver sensor. The SNR of the received signal depends on the power of the transmitter, the attenuations, and the bandwidth of the receiver. The distance is the major factor of attenuations. The accuracy of TDOA measurement depends on the SNR of the direct path signal received from the transmitter and the reflected signal from the target. The accuracy of AOA measurement in each sensor depends only on the SNR of the reflected signal from the target.

The direct path signal only travels between the transmitter and the receiver sensor. By high-power assumption of the transmitter (since opportunistic transmitters used in passive radar cover a large area), SNR of the received direct-path signal is desirable. The reflected signal travels from the transmitter to the target and travels from the target to the receiver sensor after reflection. This is far greater than the distance between the transmitter and the receiver sensor. This signal also has additional major attenuation due to the target RCS.

According to the signal model, the SNR of the echo signal increases by a decrease of the distance of the receiver to the target location. Therefore, by reduction of the distance of the receiver to the target location, the accuracy of measurements increases and σ is decreased (i.e. $\sigma\sim 1/r_{Ta-Rx_j}$). As is clear, a decrease in σ increases FIM and decrease CRLB.

Derivative of the Measurement

According to Eq. (8), the Derivatives of the measurements are inversely related to the distance of the receiver to the target location. Therefore, the Derivatives of the measurements increase by a decrease of the distance of the receiver to the target location. As is clear, an increase in Derivative increases FIM and decrease CRLB.

Optimum Arrangement

The locations that can be used to place receiver sensors are practically limited. The $\{\underline{p}_{Rx}\}$ indicates a set of the possible locations for receiver sensors. The optimal arrangement is equal to selecting N location from $\{\underline{p}_{Rx}\}$ to place the receiver sensors. It is clear that each arrangement compared to other arrangements has better performance in some locations and worse performance in some others. Therefore, there isn't an optimum arrangement that maximizes efficiency for all locations. Therefore, the set of important target locations for surveillance must be determined first. The $\{\underline{p}_{Ta}\}$ indicates the set of these locations. Then average performance at these points is optimized.

The optimal arrangement for the target localization is achieved by minimizing the average CRLB in the set of important target locations. First, we calculate the average CRLB for important target locations of each arrangement. Then, the optimal arrangement is the arrangement that minimizing the average CRLB. This arrangement maximizes the target location estimation accuracy on these important target locations. The optimal arrangement is obtained by solving the $\{\underline{p}_{Rx}\}_{opt}=argmin_{\{\underline{p}_{Rx}\}}\sum_k CRLB(\underline{p}_{Ta_k});\ \underline{p}_{Ta_k}\in\{\underline{p}_{Ta}\}$ equation using the search method on all possible locations of the receiver sensors.

Simulation

In this section, we present the simulation results of different processing scenarios. The lower band of RMSE (Root Mean Square Error) of the target location estimation is provided by the square root of CRLB. The provided RCRLB denotes the distance and the meter as its unit. Simulation results are shown by the colored contours on a two-dimensional plane. The simulations are presented in two different categories. The first category illustrates the impact of the measurements and the number of transmitters on the performance. The second category illustrates the sensors arrangement effect on the performance. In all simulations, the RCRLB is illustrated in the space, including $x=[-150\ km\ 150km]$, $y=[-10\ km\ 300\ km]$, and the target height is $9\ km$. The locations of the transmitters, receiver sensors location for the linear arrangement, and semicircular arrangement of the receiver sensors are presented in Table 1. The value

Table 1—Positions of the transmitters and receiver sensors

x	y	z	sensor	
0 km	0 km	200 m	1	
20 km	20 km	100 m	2	Transmitters
-20 km	20 km	100 m	3	
0 km	L km	200 m	1	Receiver sensors in
L km	L km	100 m	2	the linear
-L km	L km	100 m	3	arrangement
- L km	0 km	100 m	1	Sensors in the
0 km	L km	200 m	2	semicircular
L km	0 km	100 m	3	arrangement

of L for two different range arrangements of the receiver sensors is 10 Km for closed arrangement and 30 Km for distant arrangement.

In these figures, the standard deviations of the TDOA measurements noises are 100 ns, the azimuth DOA measurements' noises are 1 deg, and the elevation DOA measurements' noises are 3 deg. For simplicity, we consider the accuracy of TDOA and AOA measurements to be constant in all of the areas. Because the purposes are investigation of the effects of the integration of measurements and of alignment of sensors, all results can be generalized without losing the generality.

The impact of the measurements and the number of opportunistic transmitters are shown in Fig. 1. The RCRLB value is shown for the first transmitter of the Table 1 in figures Fig. 1 a, Fig. 1c, and Fig. 1e and for 3 transmitters of the Table 1 in figures Fig. 1b, Fig. 1d, and Fig. 1f. These figures show the RCRLB value for TDOA measurements alone in figures Fig. 1a and Fig. 1b, DOA measurements alone in figures Fig. 1c and Fig. 1d, and combined use of TDOA and DOA measurements in figures Fig. 1e and Fig. 1f. The locations of the receiver sensors are according to the linear arrangement of Table 1 and sensors are considered at close range in Fig. 1. As mentioned, the value of L, in this case, is assumed to be 10 Km.

As shown in Fig. 1, the use of TDOA measurements has a blind area (Fig. 1a), which is eliminated by increasing the number of transmitters (Fig. 1 b). Increasing the number of transmitters causes an increase in the number of bistatic pairs per sensor. These zones will appear along the line of the sensors in Fig. 1 a. The accuracy performance of the target location estimation has almost tripled by the increasing number of transmitters from 1 to 3 (compare Fig. 1a with

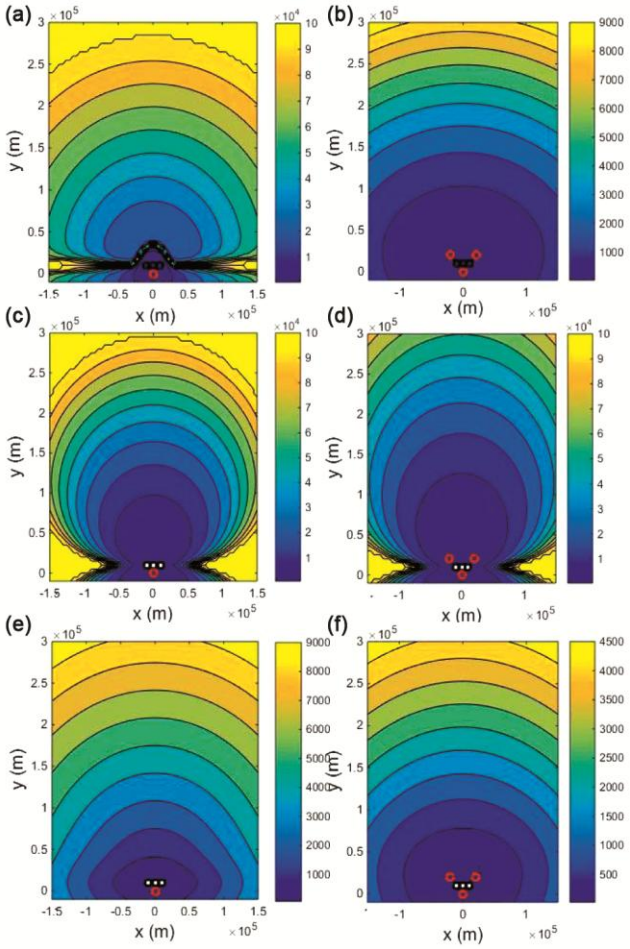

Fig. 1—RCRLB on the two-dimensional plane X and Y for 3 linear arrangement receiver sensors at close range by the use of a) only TDOA measurements and one transmitter, b) only TDOA measurements and 3 transmitters, c) only AOA measurements and one transmitter, d) only AOA measurements and 3 transmitters, e) TDOA and AOA measurements together and one transmitter, and f) TDOA and AOA measurements together and 3 transmitters

Fig. 1b). The use of DOA measurements provides the uniform semicircular accuracy area around the sensors (Fig. 1c and Fig. 1d). In the use of DOA measurements, the efficiency decreases sharply with the increasing range. The use of DOA measurements also has blind areas that cannot be eliminated even by the increasing number of transmitters (Fig. 1c and Fig. 1d). As it is shown in the figures Fig. 1e and Fig. 1f, the combined use of measurements greatly improves the performance and also eliminates the blind areas (compare Fig. 1e and f with Fig. 1a, b, c, and d).

In Fig. 2 the RCRLB efficiency for the combined use of DOA and TDOA measurements for the linear

arrangement of the receiver sensors are shown in the Fig. 2a and Fig. 2b, and semicircular arrangement are shown in the Fig. 2c and Fig. 2d. Locations of the 3 considered transmitters are according to 3 transmitters in the Table 1 and locations of the receiver sensors are according to the linear arrangement of the Table 1 and the semicircular arrangement of the Table 1. In these figures, the distances of the receiver sensors are considered at close distance (L equal to 10 Km) in the figures Fig. 2a and Fig. 2c and in the far distance (L equal to 30 Km) in the figures Fig. 2b and Fig. 2d.

As illustrated above, increasing the distances of the receiver sensors improves the efficiency (compare Fig. 2a with Fig. 2 b and compare Fig. 2c with Fig. 2 d) but the need of the reference signals of the transmitters is the limiting factor. On the other hand, the performance precision depends on the arrangement of the sensors.

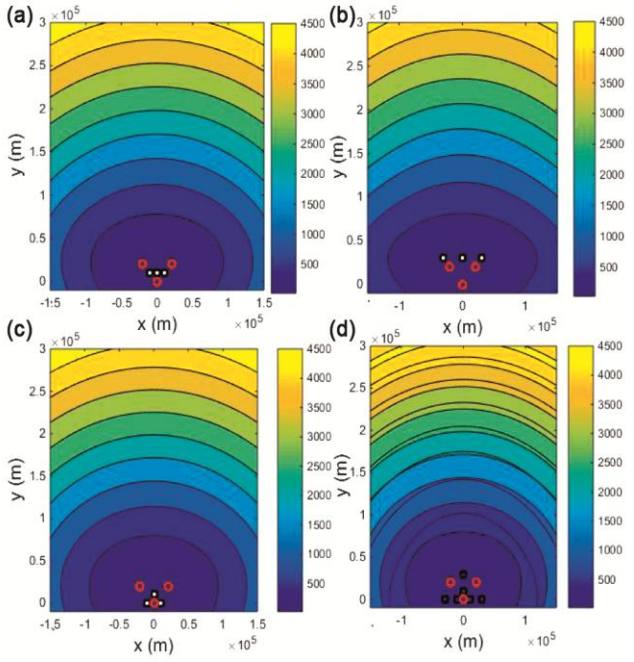

Fig. 2—RCRLB on the two-dimensional plane X and Y for use of TDOA and AOA measurements together by 3 transmitters and a) 3 linear arrangement receiver sensors at close range, b) 3 linear arrangement receiver sensors at far range, c) 3 semicircular arrangement receiver sensors at close range and d) 3 semicircular arrangement receiver sensors at far range

For transparency, a numerical example is presented in Table 2. This table presents the value of RCRLB for 3 different points of figures. The first point ($\underline{P}_{Ta}$=[*150 km 5 km 9 km*]^T) is part of blind areas, the second point ($\underline{P}_{Ta}$=[*15 km 15 km 9 km*]^T) is close to sensors, and the third point ($\underline{P}_{Ta}$=[*15 km 150 km 9 km*]^T) is long distant from sensors. As mentioned in the past paragraphs for Fig. 1 and Fig. 2 descriptions, the presented conclusions are clear for increasing the distance between sensors and increasing the number of transmitters.

The target height effect on the efficiency is shown in the Fig. 3. Here Fig. 3a indicates the target in a position ($\underline{P}_{Ta}$=[*15 km 50 km h*]^T) at a medium distance from the sensors and Fig. 3b indicates the target in a position ($\underline{P}_{Ta}$=[*15 km 150 km h*]^T) at a long distance from the sensors. In these figures, *h* is according to the axis of the figures. As illustrated, the target height effect is low on performance, especially in multi-transmitter modes.

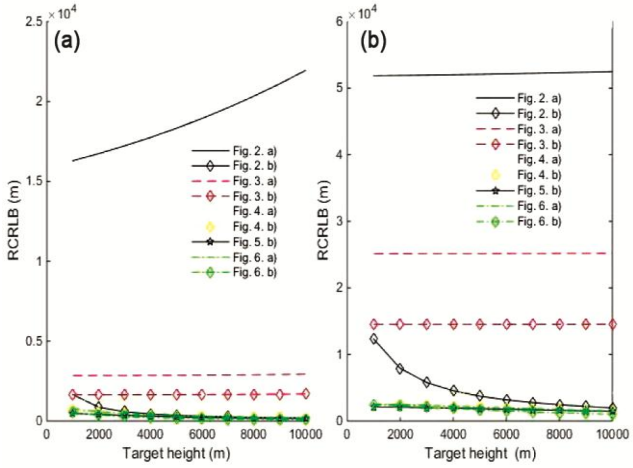

Fig. 3—RCRLB for different target height for the target in a position at the a) medium-range and b) far range

Table 2—RCRLB for 3 points of figures

Fig. 1						Fig. 2				Point
a	b	c	d	e	f	a	b	c	d	
100km<	1.3 km	100 km<	100 km<	3.7 km	1.2 km	1.2 km	839 m	1.2 km	802m	Blind area
2.1km	257m	2.9km	1.6 km	1.3 km	200m	200m	167 m	191m	99m	Near point
52.4km	2.1 km	25.1 km	14.5 km	4.2 km	1.6 km	1.6 km	1.5 km	1.6 km	1.1 km	Far point

Conclusions

In this paper, the effect of receiver sensors arrangement is investigated on the performance of the passive radar. The Cramer-Rao lower band of the target location estimation is presented. The presented CRLB utilizes DOAs as like as TDOAs. The presented CRLB depends on the accuracy of the measurements and the locations of the transmitters, receivers, and Target and is independent of the signal features. As illustrated, there are blind areas in the estimation of the target location by the use of TDOA or AOA measurements individually. These blind areas depend on the arrangement of the sensors. The blind areas are eliminated by utilizing DOA and TDOA together and the accuracy of estimation of the target location is greatly enhanced. The efficiency improves to approximately the same rate by increasing the distance between the sensors and decrease distances of them to the target location. However, the limiting factor is the need to receive signals of the transmitters. The proposed method causes maximum target localization accuracy on the important target locations by the optimal arrangement of the receiver sensors in the set of possible locations for a specific set of opportunistic transmitter.

References

1 Willis N & Griffiths H D, *Advances in Bistatic Radar* (Scitech Pub Inc.) 2007.

2 Griffiths H D, Baker C J, *An Introduction to Passive Radar* (Artech House) 2017.

3 Cherniakov M, *Bistatic Radar: Emerging Technology* (JohnWiley& Sons Ltd) 2008.

4 Silent Sentry®. Innovative Technology for Passive, Persistent Surveillance, *Lockheed Martin* (2007).

5 KuschelH, Cristallini D, Olsen K E, Tutorial: Passive radar tutorial, *IEEE Aerosp Electron Syst Mag*, **34** (2019) 2–19.

6 Ingenious Inventions – Radar, *Sci Rep*, **50(11)** (2013) 53.

7 Jain A R, Rao P B, Rao Y J, Radar signal spectra dependence on the pulse width: Observations using ST mode of the Indian MST radar, *Indian J Radio Space Phys*, **23(1)** (1994) 86–92.

8 Glende M, Heckenbach J, Kuschel H, Müller S, Schell J, Schumacher C, Experimental passive radar systems using digitalilluminators (DAB/DVB-T), in *Proc The 2014 15th Int Radar Symp (IRS)* 5–7 September 2007.

9 Zemmari R, Broetje M, Battistello G, Nickel U, GSM passivecoherent location system: Performance prediction and measurement evaluation, *IET Proc Radar, Sonar Navig*, **8** (2014) 94–105.

10 Colone F, Falcone P, Bongioanni C, Lombardo P, WiFi-based passive bistatic radar: Data processing schemes and experimental results, *IEEE Trans Aerosp Electron Syst*, **48** (2012) 1061–1079.

11 He X, Zeng T, Cherniakov M, Signal detectability in SS-BSARwith GNSS non cooperative transmitter, *IEE Proc—Radar Sonar Navig*, **152** (2005) 124–132.

12 Wang J, Qin Z, Gao F, Wei S, An Approximate Maximum Likelihood Algorithm for Target Localization in Multistatic Passive Radar, *Chin J Electron*, **28(1)** (2019) 195–201.

13 Huang J H, Garry J L, Smith G E, Array-based target localisation in ATSC DTV passive radar, *IET Radar, Sonar Navig*, **13(8)** (2019) 1295–1305.

14 Zhang S, Huang Z, Feng X, He J, Shi L, Multi-sensor passive localization using second difference of coherent time delays with incomplete measurements, *IEEE Access*, **7** (2019) 43167–43178.

15 Huang J H, Garry J L, Smith G E, Array-based target localisation in ATSC DTV passive radar, *IET Radar, Sonar Navig*, **13(8)** (2019) 1295–1305.

16 Wang J, Qin Z, Wei S, Sun Z, Xiang H, Effects of nuisance variables selection on target localisation accuracy in multistatic passive radar, *Electron Lett*, **54(19)** (2018) 1139–1141.

17 Hack D E, Patton L K, Himed B, Saville M A, Detection in Passive MIMO Radar Networks, *IEEE Trans Signal Process*, **62(11)** (2014) 2999–3012.

18 Hack D E, Patton L K, Himed B, Saville M A, Centralized Passive MIMO Radar Detection Without Direct-Path Reference Signals, *IEEE Trans Signal Process*, **62(11)** (2014) 3013–3023.

19 TalariS F, Mohamedpour K, Efficiency of Target Location Scenarios in theMulti-Transmitter Multi-Receiver Passive Radar, *Int J Nonlinear Anal Appl*, **10(1)** (2020) 217–228.

20 Kay S M, *Fundamentals of Statistical Signal Processing: Estimation theory* (Prentice-Hall) 2007.